Supplemental Materials for "Robust Empirical Bayes Confidence Intervals"

Timothy B. Armstrong[*]   Michal Kolesár[†]

Yale University   Princeton University

Mikkel Plagborg-Møller[‡]

Princeton University

April 7, 2020

Appendix C   Empirical appendix

This Supplemental Appendix provides further results and details for the neighborhood effects application in Section 6.1 and the factor model application in Section 6.2.

C.1   Neighborhood effects

Figure S1 gives a plot analogous to that in Figure 6, but for children with parents at the 75th percentile of the income distribution. Since the signal-to-noise ratio is lower here, the EB estimates shrink Y_i more aggressively towards the regression line.

Figure S2 gives a plot of the density of the t-statistics $Y_i/\hat{\sigma}_i$, with a normal density overlaid. It is clear from the figure that the right tail has more mass than the normal density, which explains the high kurtosis estimates in Table 1.

[*]email: `timothy.armstrong@yale.edu`
[†]email: `mkolesar@princeton.edu`
[‡]email: `mikkelpm@princeton.edu`

C.2 Structural change in the Eurozone

We first describe the data set. Then we show a histogram of the loading break t-statistics. Finally, we display the full set of estimated breaks and corresponding EBCIs, including results that impose independence between break magnitudes and standard errors.

Tables S1 and S2 list the countries and variables in the data set, respectively. If not already seasonally adjusted, we apply the X13-ARIMA-SEATS seasonal adjustment procedure to all variables other than asset prices. In the pre-2008 sample, 4.2% of the observations are missing (24% of series have at least one missing observation). We impute the missing observations in the way suggested by Stock and Watson (2016, section 2.3.4.1): First, we estimate a DFM on the non-missing data, then we regress the series with missing observations on the newly obtained principal components and impute the missing observations using this regression, then we go back and re-estimate the DFM on the now-balanced panel, then we re-impute the originally missing observations through regressions on the new factors, and so on until numerical convergence. For simplicity, we ignore any error induced by the imputation.

Figure S3 shows the t-statistics for the estimated loading breaks. We remark that the shape is consistent with an approximately normal underlying distribution of breaks divided by standard errors.

Figures S4 to S7 show the shrinkage-estimated loading breaks and 95% robust EBCIs for the remaining series not already shown in Figure 7. Notice that none of the series exhibit as marked a tendency of breaking in one direction (given the estimation uncertainty indicated by the EBCI) as the government bond spread and stock price index in Figure S8. However, a few other systematic results are worth noting. CPI inflation changes in several countries have generally become less correlated with the area-wide cycle (it was positively correlated with the area-wide cycle in the pre-break period in almost all countries). Household and non-financial business credit growth has similarly generally become less correlated with the area-wide cycle in most countries, although this change is somewhat harder to interpret, since the signs of the pre-break loadings are quite heterogeneous across countries.

Figures S8 to S12 shows the estimated breaks and robust EBCIs using t-statistic shrinkage (cf. Remark 3.8) which avoids imposing the assumption of cross-sectional moment independence between break magnitudes and standard errors at the cost of not guaranteeing valid EB coverage *conditional* on the standard errors (cf. Remark 3.2). Notice that the figures are similar to Figures S4 to S7 and 7, which did impose moment independence.

References

Stock, J. H. and Watson, M. W. (2016). Factor Models and Structural Vector Autoregressions in Macroeconomics. In Taylor, J. B. and Uhlig, H., editors, *Handbook of Macroeconomics*, volume 2, pages 415–525. Elsevier.

Table S1: Countries in the dataset used in the Eurozone DFM application.

Code	Country	#series
AT	Austria	13
BE	Belgium	13
CY	Cyprus	8
DE	Germany	12
EE	Estonia	9
ES	Spain	13
FI	Finland	13
FR	France	13
GR	Greece	12
IE	Ireland	13
IT	Italy	13
LT	Lithuania	10
LU	Luxembourg	12
LV	Latvia	9
MT	Malta	8
NL	Netherlands	13
PT	Portugal	12
SI	Slovenia	10
SK	Slovakia	7
EZ	Eurozone	8

Notes: The last row lists the number of Eurozone-wide series. The last column lists the number of country-specific series.

Table S2: Variables in the data set. Code: series codes used in Figure 7 and Figures S4 to S7

Code	Series	Source	Stat. transf.	#countries
CA	current account divided by GDP	Eurostat	Δ	16
CAPUTIL	capacity utilization	Eurostat	none	18
CONS	real consumption	Eurostat	Δlog	18
CONSCONF	consumer confidence index	Eurostat	none	19
CPI	consumer price index	Eurostat	Δ^2log	19
CREDITHH	credit to households divided by GDP	BIS	Δlog	12
CREDITNFB	credit to non-fin. bus. divided by GDP	BIS	Δlog	12
EUR	euro exchange rate	Eurostat	Δlog	5 currencies
GDP	real GDP	Eurostat	Δlog	18
GOVBOND	10-yr gov't rate vs. 3-month EZ rate	Eurostat	Δ	18
HOUSEP	nominal house price index	BIS	Δlog	11
INT3M	3-month EZ interest rate	Eurostat	Δ	1 (EZ)
INTDD	overnight EZ interest rate	Eurostat	Δ	1 (EZ)
OILBRENT	Brent crude oil price	U.S. EIA	Δlog	1 (EZ)
STOCKP	stock price index	OECD	Δlog	15
UNEMPRATE	unemployment rate	Eurostat	none	19
WAGE	nominal wage index	Eurostat	Δlog	18

Notes: Stat. transf.: stationarity transformation method. The five euro exchanges rates are against the Swiss Franc (CHF), Chinese Yuan (CNY), British Pound (GBP), Japanese Yen (JPY), and United States Dollar (USD).
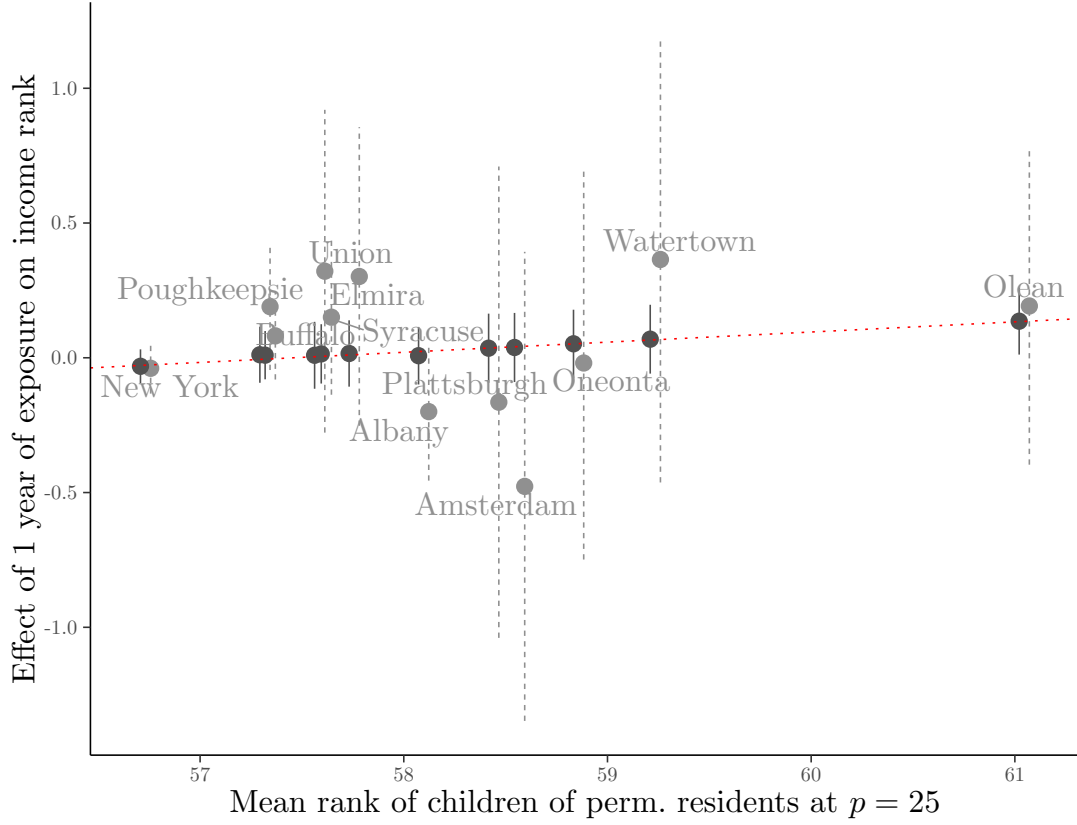
Figure S1: Neighborhood effects for New York and 90% robust EBCIs for children with parents at the $p = 75$ percentile of national income distribution, plotted against mean outcomes of permanent residents. Dashed gray lines correspond to CIs based on unshrunk estimates, and solid black lines correspond to robust EBCIs based on EB estimates that shrink towards a dotted regression line based on permanent residents' outcomes. Baseline implementation.
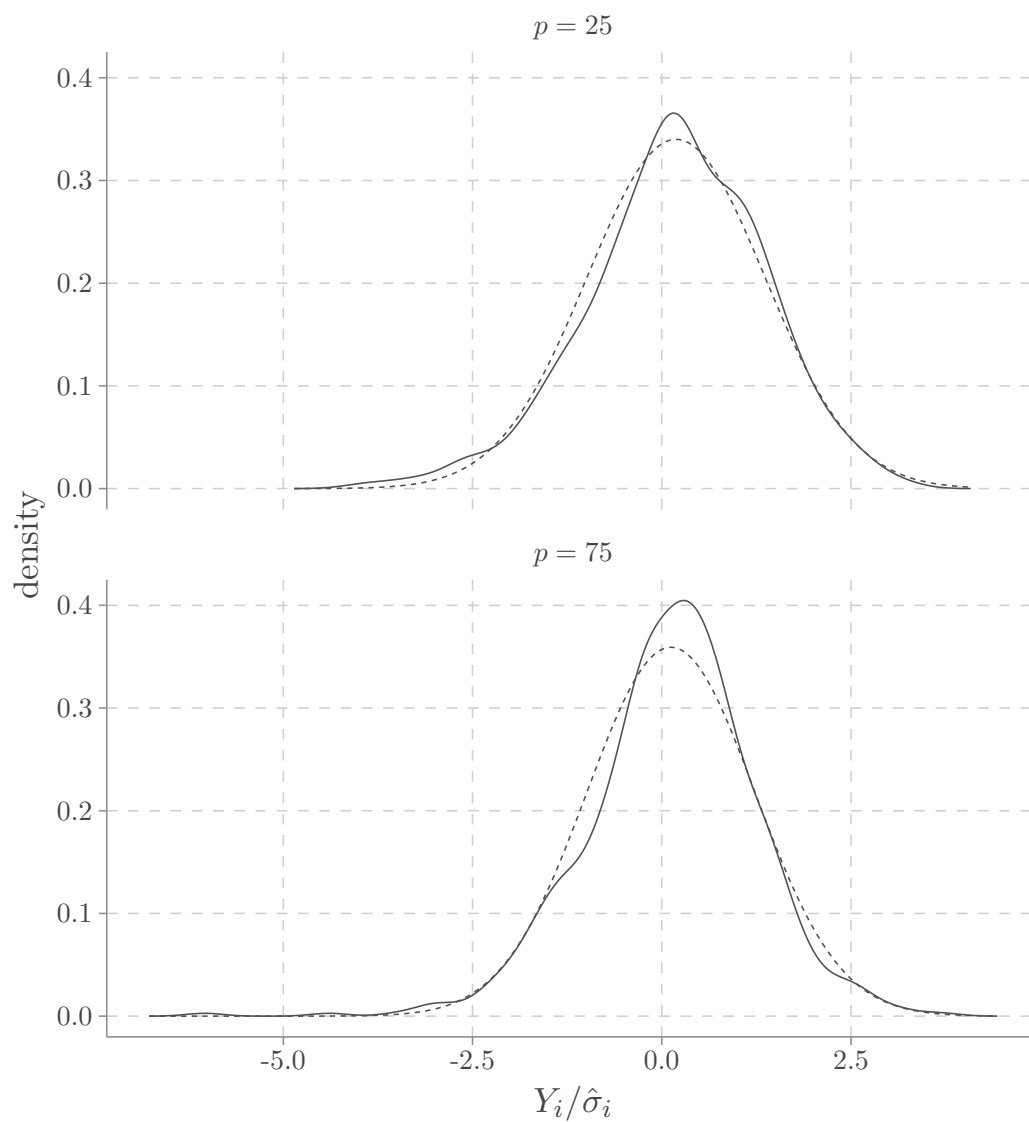
Figure S2: Estimated density of t-statistics $Y_i/\hat{\sigma}_i$ for neighborhood effects for children with parents at the $p = 25$ and $p = 75$ percentile of national income distribution. Dashed line overlays a normal density. Bandwidth selected using the Silverman rule of thumb.
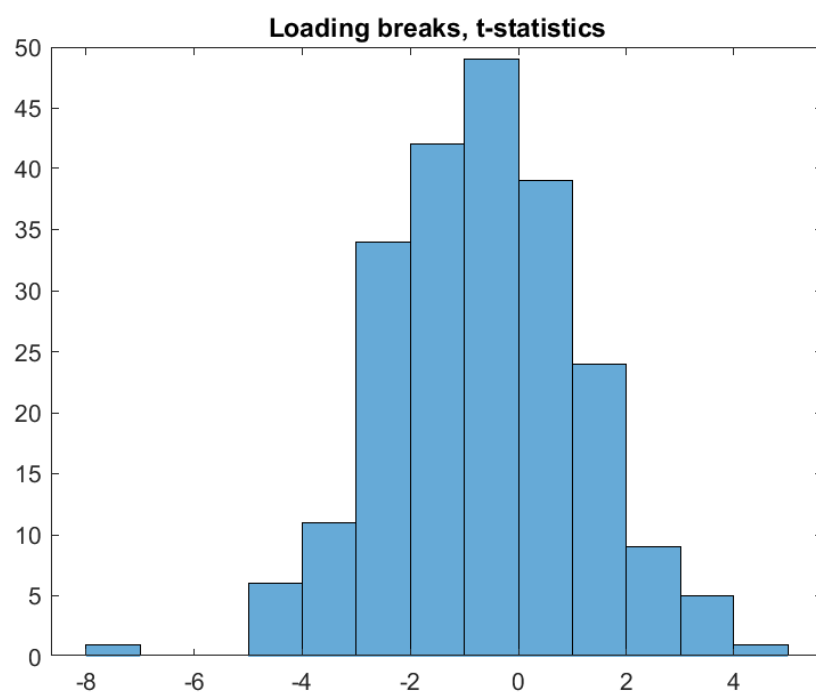
Figure S3: Histogram of t-statistics $Y_i/\hat{\sigma}_i$ for loading breaks.
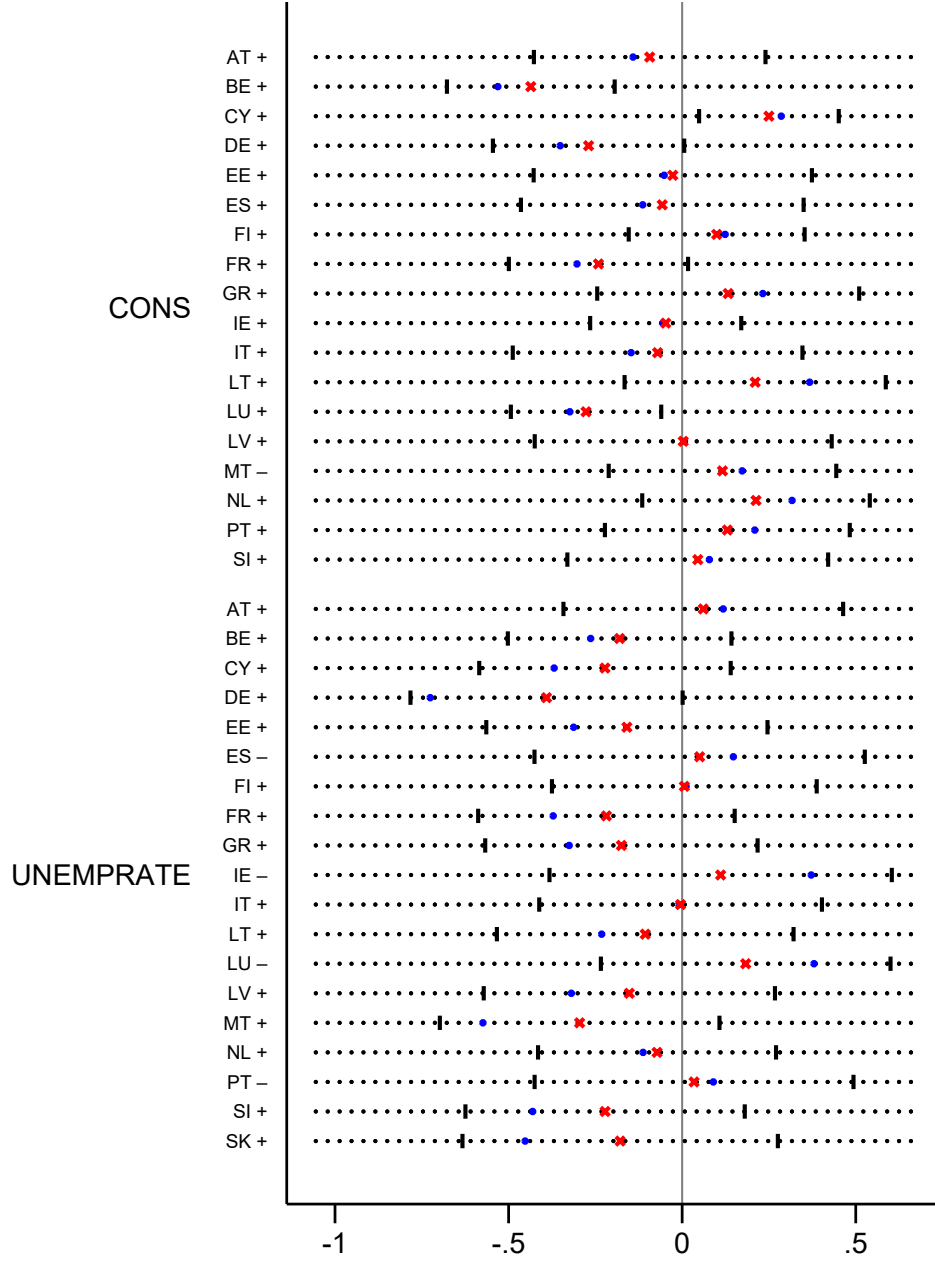
Figure S4: Estimated loadings and 95% robust EBCIs as in Figure 7, but here for real consumption growth (CONS) and the unemployment rate (UNEMPRATE).
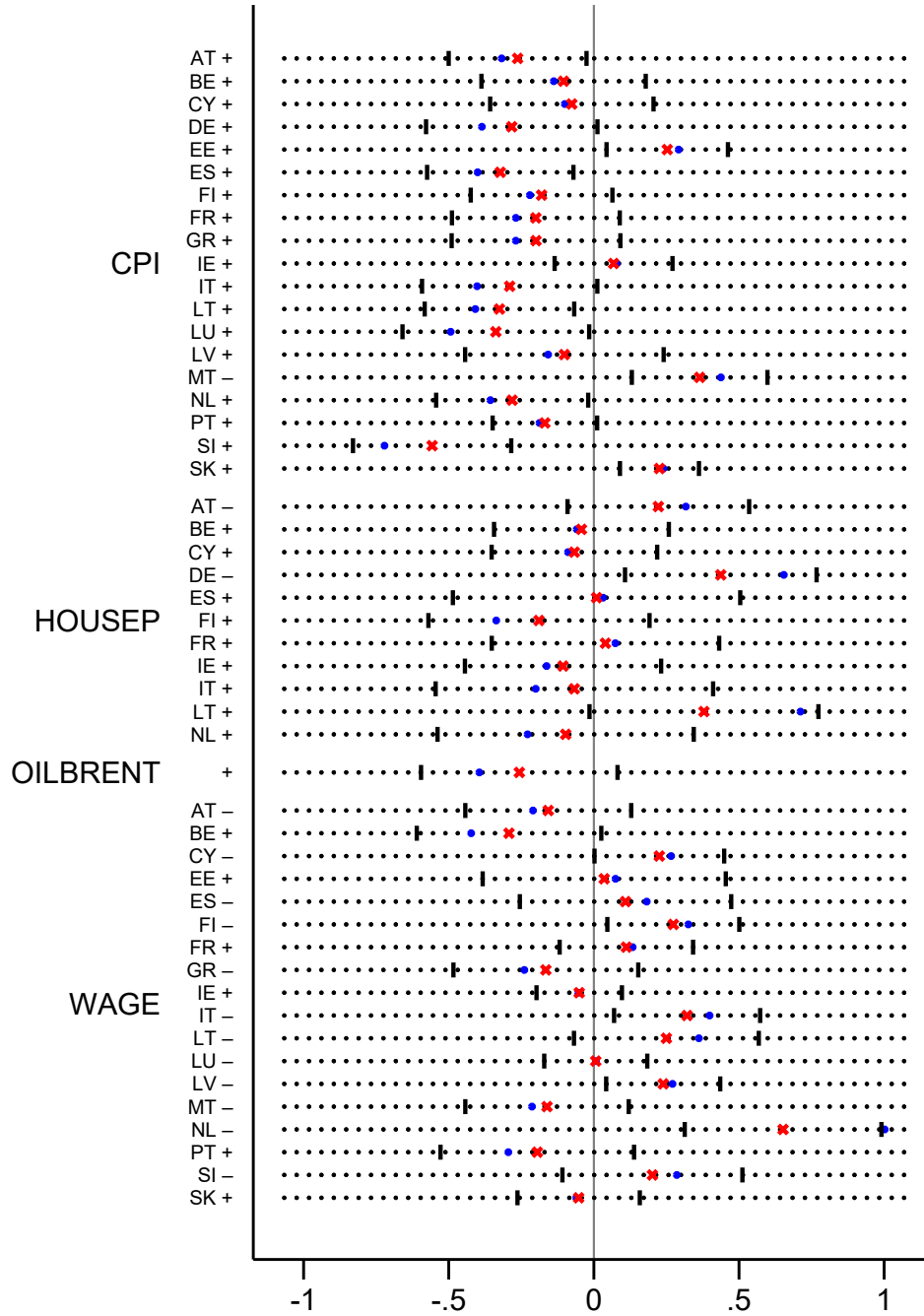
Figure S5: Estimated loadings and 95% robust EBCIs as in Figure 7, but here for changes in CPI inflation (CPI), house price growth (HOUSEP), Brent crude oil price growth (OIL-BRENT), and wage growth (WAGE).

10
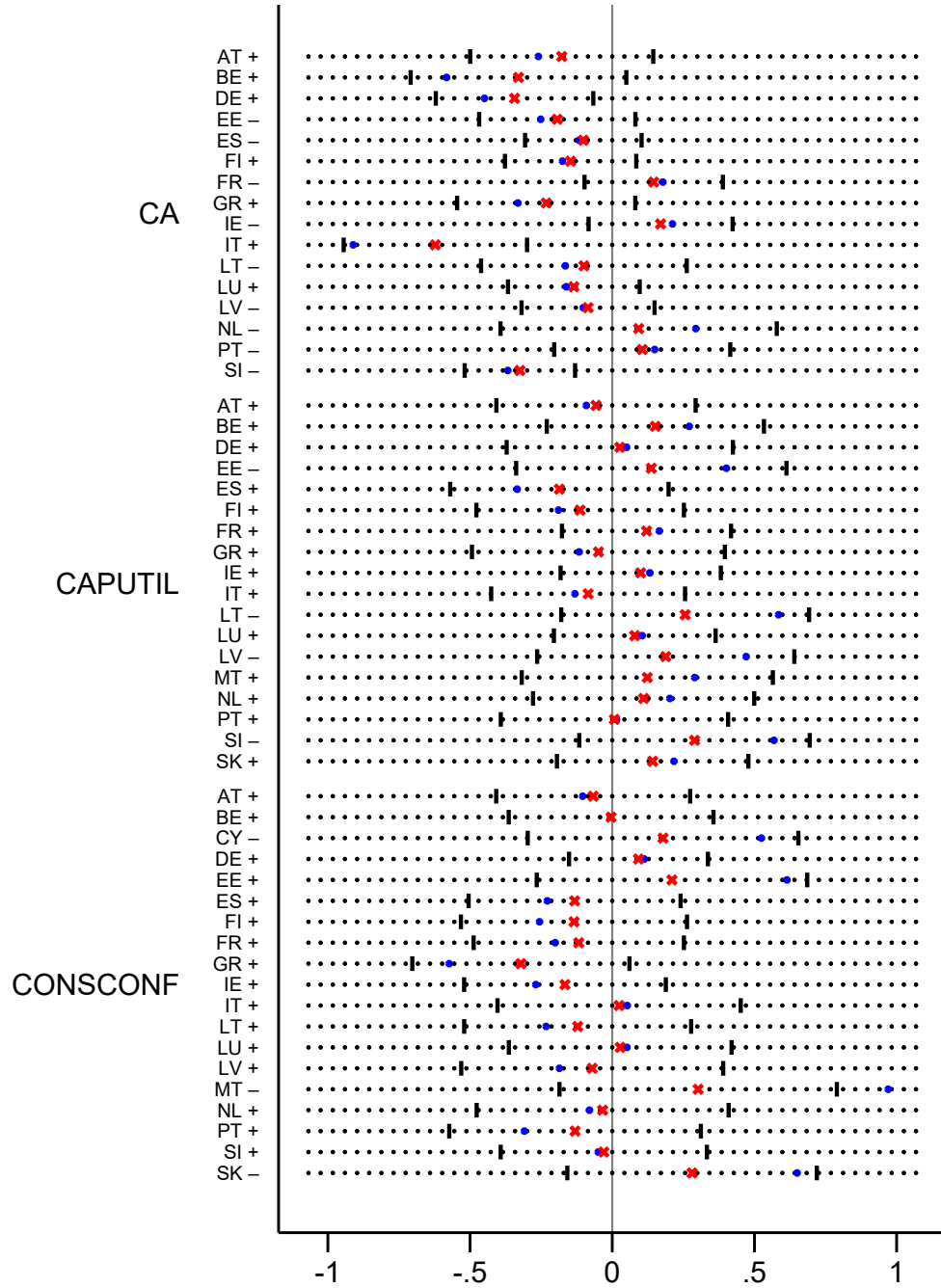
Figure S6: Estimated loadings and 95% robust EBCIs as in Figure 7, but here for changes in the current account divided by GDP (CA), capacity utilization (CAPUTIL), and consumer confidence index (CONSCONF).
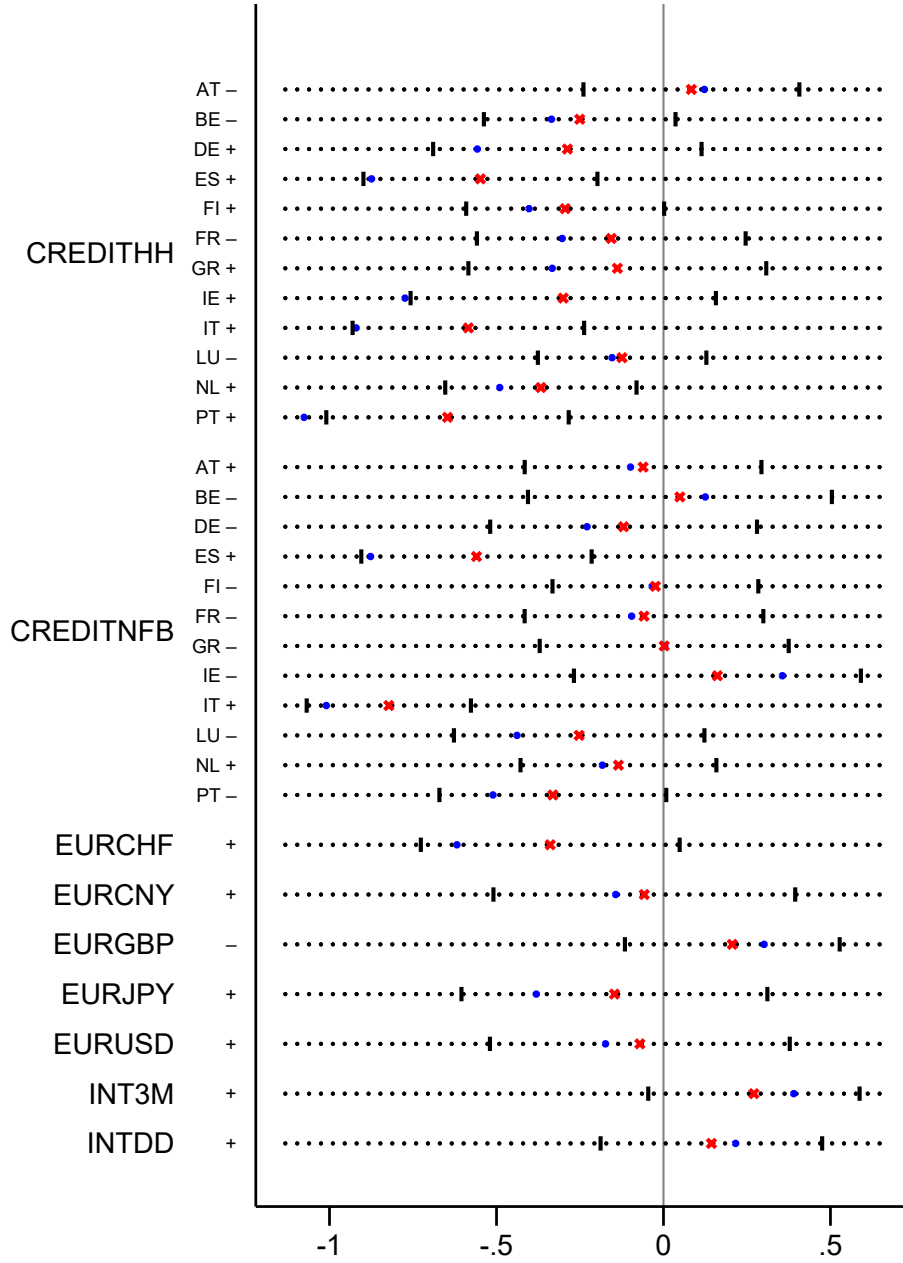
Figure S7: Estimated loadings and 95% robust EBCIs as in Figure 7, but here for growth in credit to households (CREDITHH) and to non-financial businesses (CREDITNFB), log changes in euro exchange rates measured in foreign currency per euro (EUR), and changes in short-term interest rates (INT3M: 3-month, INTDD: overnight).
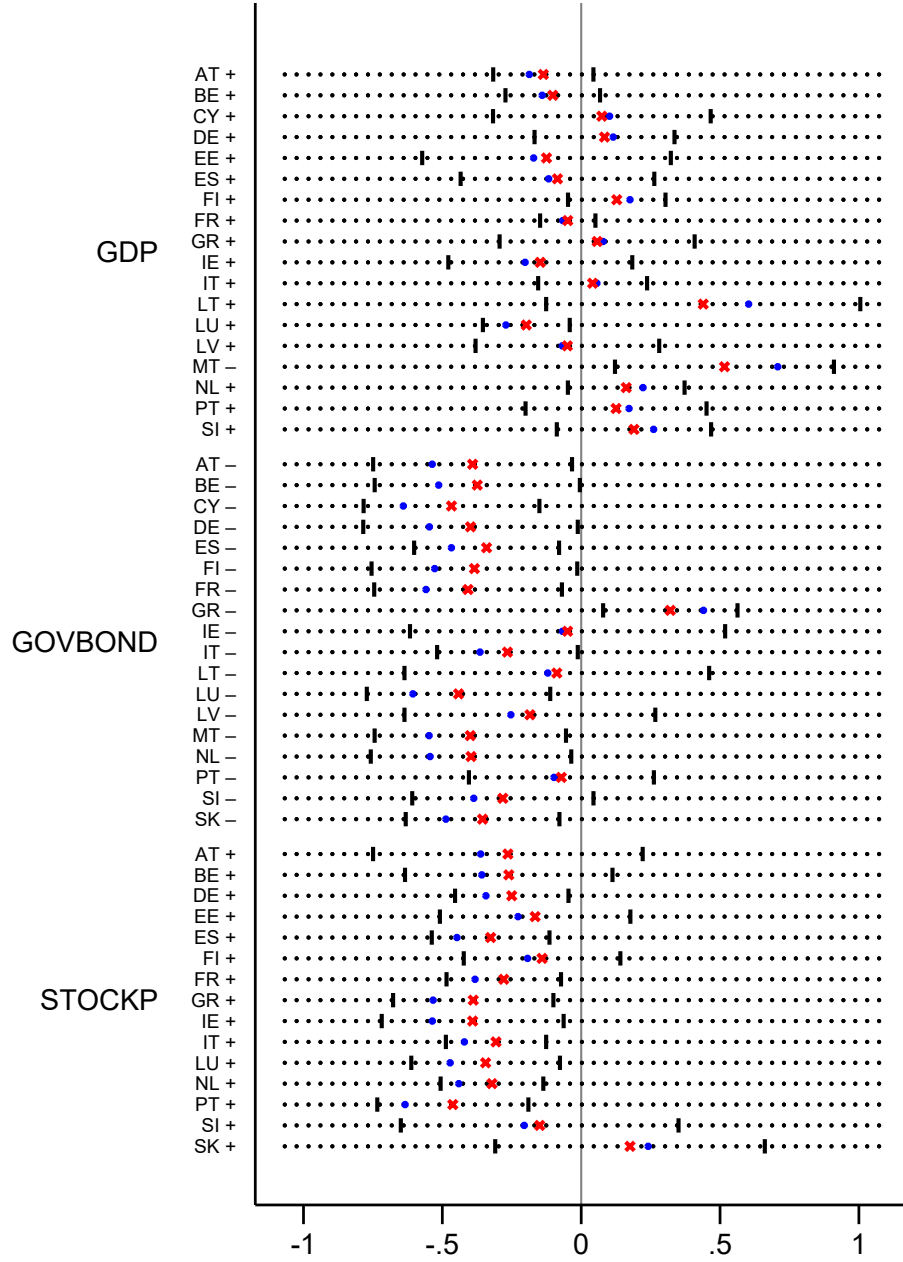
Figure S8: Estimated loadings and 95% robust EBCIs as in Figure 7, but here using t-statistic shrinkage.
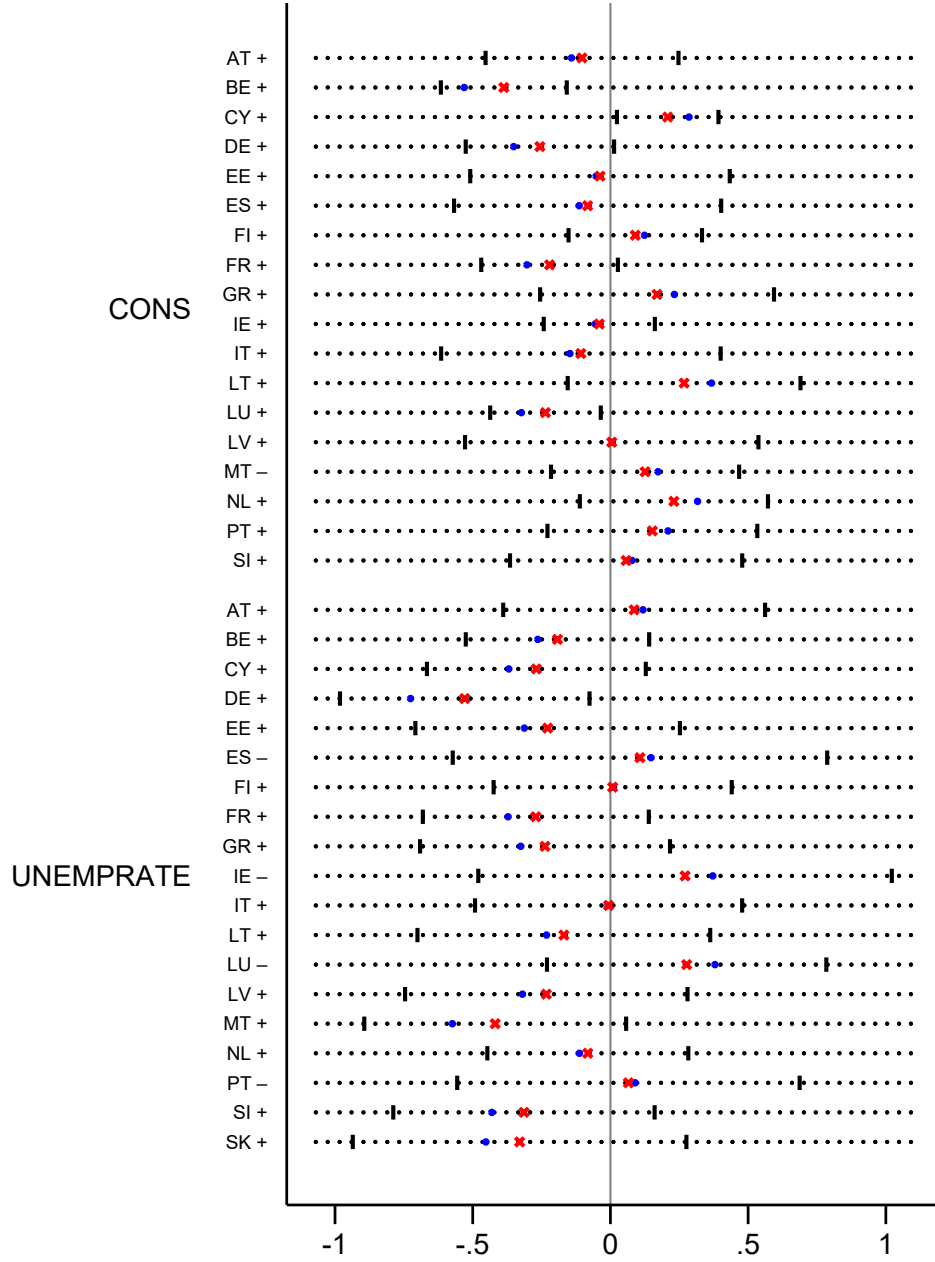
Figure S9: Estimated loadings and 95% robust EBCIs as in Figure S4, but here using t-statistic shrinkage.
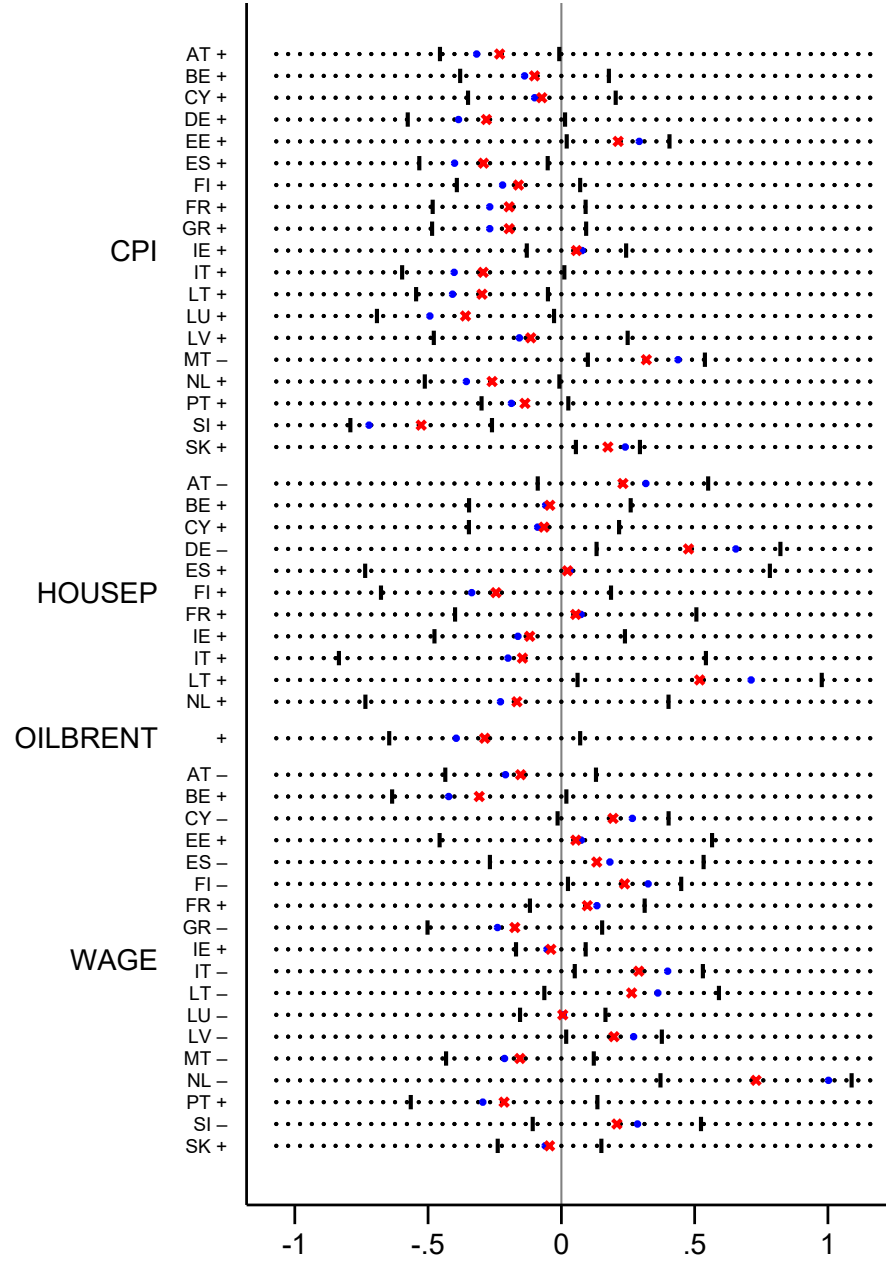
Figure S10: Estimated loadings and 95% robust EBCIs as in Figure S5, but here using t-statistic shrinkage.
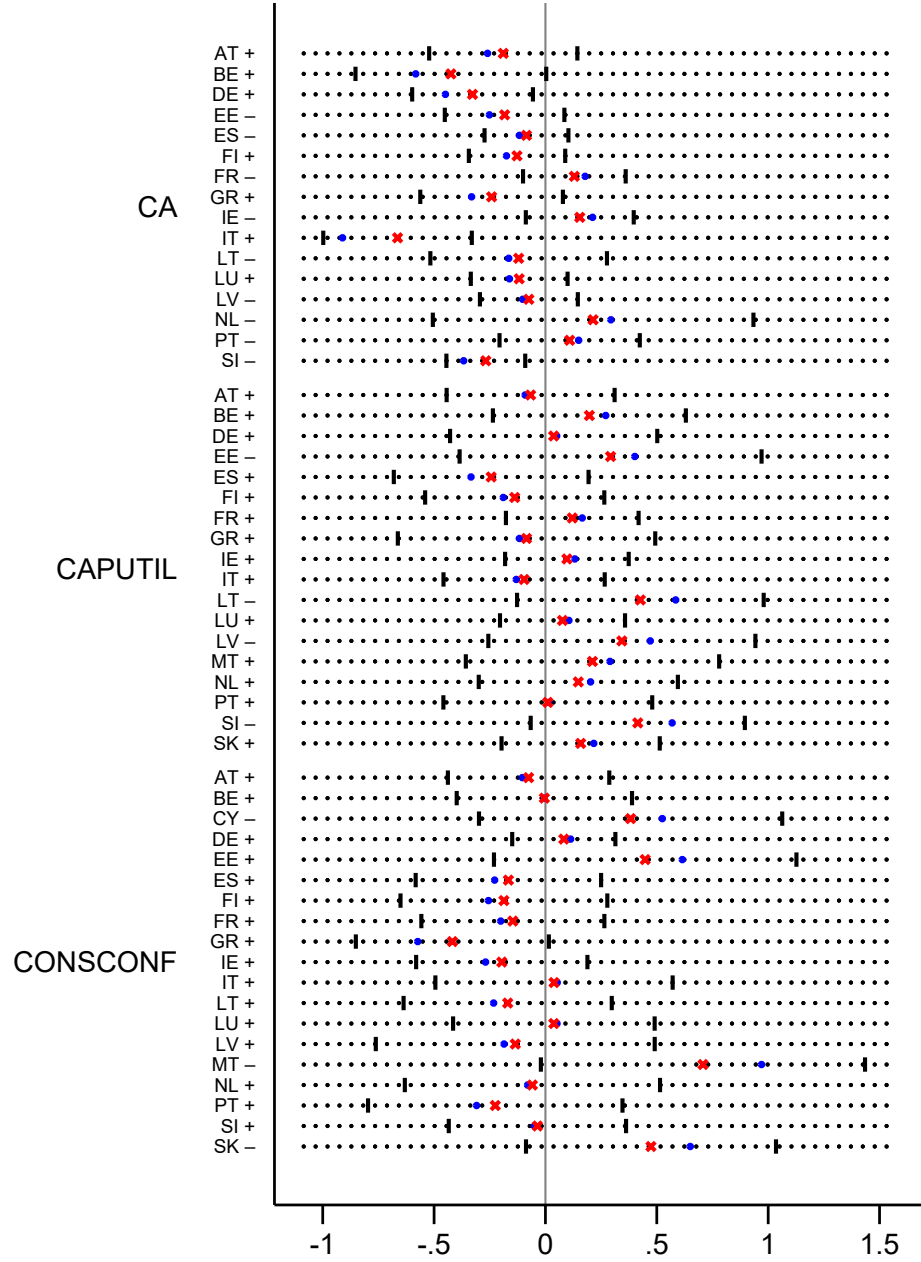
Figure S11: Estimated loadings and 95% robust EBCIs as in Figure S6, but here using *t*-statistic shrinkage.
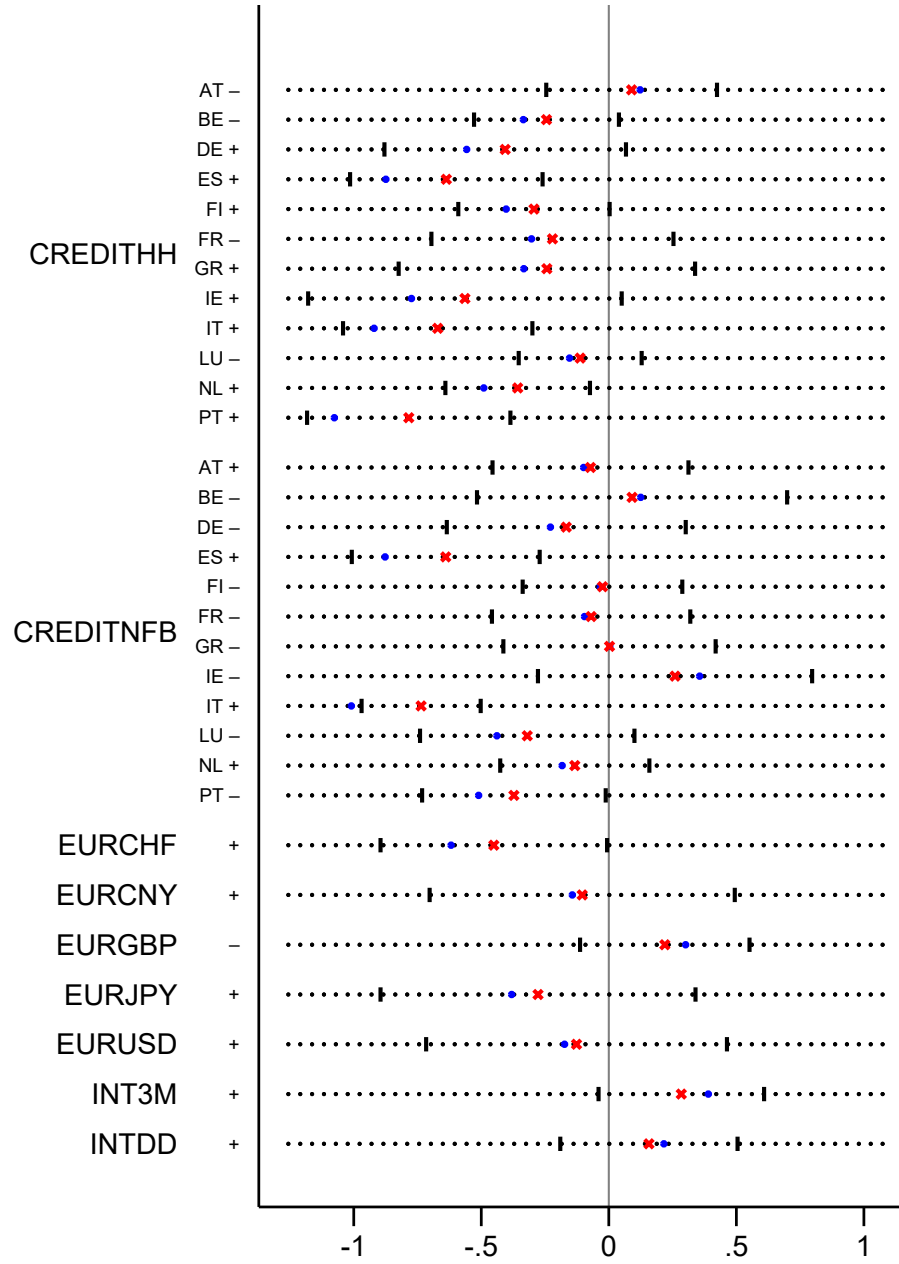
Figure S12: Estimated loadings and 95% robust EBCIs as in Figure S7, but here using t-statistic shrinkage.